# Field Axial Testing of Screw Micropiles in Sand and SPT-based Estimation Method

Mujtaba Khidri, Lijun Deng
*Department of Civil and Environmental Engineering*
*University of Alberta, Edmonton, Alberta, Canada*

ABSTRACT
A screw micropile consists of a smooth shaft segment, one or two threaded shaft segments and one or two threaded-tapered shaft segments. Field test research is required to investigate the axial capacity and shaft resistance distribution of the pile in sand. Axial compression and tension tests were performed on screw micropiles installed at a sand site near Edmonton, Alberta. The diameters of the test piles were 76 mm, 89 mm and 114 mm and the length was 3 m. Selected piles were instrumented with strain gauges to measure load distributions along the shaft. Three axial compression load tests and three axial tension load tests were conducted for each pile type. From the load-displacement curves, the ultimate capacities of the test screw micropiles were estimated at an axial load corresponding to an axial displacement equal to 10% of shaft diameter. From strain gauge readings, axial load and shaft resistance distributions were determined. A comprehensive geotechnical site investigation was carried out to develop the soil profile and the soil parameters. Statistical relationships were developed between shaft resistance distributions and standard penetration test N value distribution using linear regression analysis. Regression coefficients were obtained for smooth, threaded, and threaded-tapered segment separately. The coefficients were used to estimate the ultimate capacities of all other screw micropiles.

## 1 INTRODUCTION

Screw micropiles have been recently introduced to the construction industry of North America. This pile type consists of a smooth, one or two threaded and threaded-tapered segment(s). It is installed using a torque head fixed on small construction equipment that is equipped to record continuous installation torque. It is suitable for lightweight structure including timber-frame construction, advertising and traffic systems, garden and landscape construction, fencing systems, and solar systems. The size, shape and installation method of the screw micropiles are different from conventional piles such as cast-in-place, driven-steel, helical or other grouted micriopiles.

Research on the geotechnical behaviour of screw micropiles is at an early stage. Guo and Deng (2018) conducted full-scale load tests of the instrumented screw micropiles in cohesive soil. The mean soil-pile adhesion coefficient was measured to be less than 0.1 due to development of an annular gap between the screw micropile and the soil. The limit load distribution of the threaded section was best represented by the cylindrical shearing mode compared to individual bearing mode. It was also found that the tapered shape increases the shaft adhesion by 143%. Guo et al. (2018) performed axial cyclic and monotonic load tests in a cohesive site (different site than Guo and Deng 2018). It was reported the adhesion coefficient of the smooth segment, threaded segment and threaded-tapered segment were 0.075, 0.85, 0.85, and 1.44, respectively. Notably, however, there is no research on the axial behavior of this new pile type in sand.

Standard Penetration Test (SPT) is very often used to estimate the axial capacities of pile foundations. For example, Shioi and Fukui (1982), Briaud et al. (1983), Meyerhof (1956), Shariatmadari et al. (2008), Shioi and Fukui (1982), Thornburn and MacVicar (1971), Aoki and Velloso (1975), Brown (2001), Decourt (1982) and Decourt (1995) performed statistical methods to develop correlation between unit shaft resistance and SPT N values for various piles.

In this paper, three types of screw micropiles were axially loaded in a sand pit site. Eight test piles were instrumented with strain gauges to measure the axial load distribution. Geotechnical drilling with SPT was performed to evaluate soil properties and profile. Unit shaft resistance distributions were obtained from strain gauge readings. Statistical relationships were developed to correlate the shaft resistance distributions with the SPT N values along the micropile shaft. Based on the developed empirical correlations, the ultimate capacities of test micropiles without strain gauges were estimated using the regression coefficient, SPT-N distribution, micropile geometry and pile penetration depth.

## 2 GEOTECHNICAL SITE INVESTIGATION

Field axial testing of screw micropiles were conducted at a sand pit site (53.8765 N, -112.9290 W) near Edmonton, AB. Before the pile tests, a geotechnical investigation consisting of four boreholes were completed using a track-mounted drill with a continuous-flight solid stem. The soil deposit in the site was comprised of Pleistocene and Holocene Aeolian sand deposit overlying lacustrine clay, which includes well-graded fine to medium grained sand (Bayrock 1958 and Fenton et al. 1983). The sand deposit was formed by the transportation of drained glacial lake beach deposits. It was generally massive to locally cross-bedded or ripple laminated with both active and vegetated dune and sand sheets. Particle size distribution were obtained from the grab sample (GS) from drill auger and split spoon (SS) sampler. Figure 1 shows the particle size distributions of GS and SS along the depths of Borehole 1 at the test site. In total, four boreholes were drilled (auger and SPT) on this sand site and a large number of sand samples were obtained.

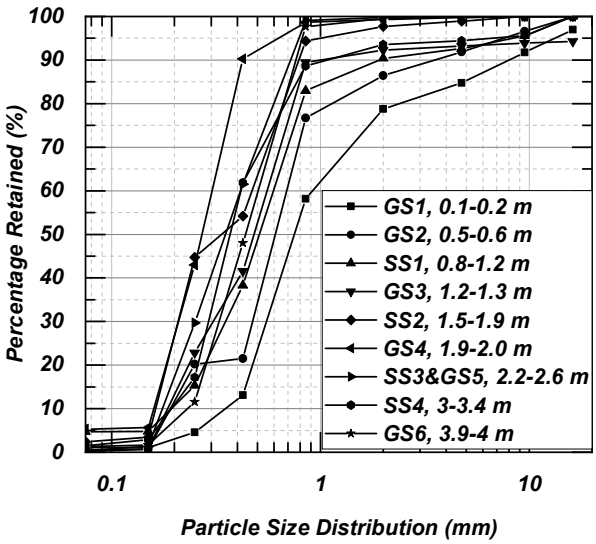


Figure 1. Particle size distribution of Borehole 1 at the test site (GS = grab samples, SS = split-spoon sample)

The sand deposit was approximately 4.3 m thick and it consisted of two distinctive sand sublayer with different composition and compactness condition. The upper 2 m of sand deposit included gravel, sand and fines with 0 to 21%, 77 to 98 %, and 0 to 5%, respectively. Grain size diameter $D_{60}$ ranged from 0.4 to 0.2 mm, with an average of 0.2 mm. The coefficient of uniformity, $C_u$ and coefficient of curvature, $C_c$ ranged from 1.9 to 4.8 and 0.5 to 1.7 respectively. The sand samples obtained from four boreholes at depth above 2 m from four boreholes were well-graded sand (SW), poorly-graded sand (SP) and well-graded sand with gravel (SW-G).

The lower 2 m of sand deposit included gravel, sand, and fines with 0 to 6.4%, 92 to 99%, and 0 to 1.6 %, respectively. Grain size diameter $D_{60}$ of all samples is 0.2 mm. The coefficient of uniformity, $C_u$ and coefficient of curvature, $C_c$ ranged from 1.8 to 2.6 and 0.6 to 1.1 respectively. The sand samples obtained from four boreholes at depth below 2 m were well-graded sand (SW) and more predominantly poor-graded sand (SP).

The moisture content (MC) in the sand varied from dry to wet with depth. The MC varied from dry to 10% in the upper sand sublayer. The MC varied from 13 to 24% in the lower sand sublayer. The groundwater table was measured to be around 1.7 to 2 m. The presence of groundwater table and pure sand contributed to greater MC at depth below 2 m. The lower sand sublayer has greater void ratio compared to the upper sand sublayer. The poor gradation of the lower sand sublayer contributes to a greater void ratio compare to the well gradation of sand with gravel. Figure 2 shows the average MC and average maximum and average minimum void ratios of sand samples of four boreholes.

SPT's were conducted at close depth interval to obtain compactness condition of the soil strata. The SPT-N value was corrected for the overburden stress. SPT $N_{1,60}$ value varies between 17 to 23 and 5 to 9 at the upper and lower sand sublayer . Four SPT's performed at four quadrants of the sandy site were used to compile an average SPT $N_{1,60}$ distribution, as shown in Figure 2. This distribution was used in the statistical analysis.

The MC profile and void ratio profile for four boreholes were consistent. The composition and compactness condition of the sand deposit was reasonably heterogeneous across the site. The coefficient of variations of SPT $N_{1,60}$ value of the sand deposit across the site at three SPT depth intervals were 0.12, 0.064 and 0.068, respectively.

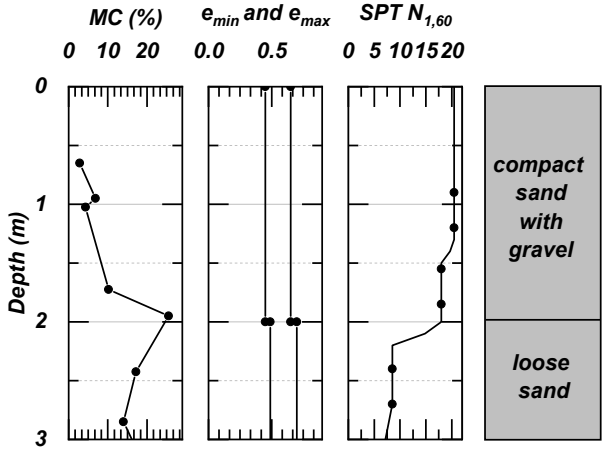


Figure 2. Profile of sand average properties of four boreholes

## 3 TEST SETUP

### 3.1 Test Pile

The test pile consisted of three types of screw micropiles: P1, P3, and P5. The test piles varied in length, diameter, and shape as shown in Table 1. The screw micropiles consisted of a smooth segment, one or two threaded segment(s) and one or two threaded-tapered segment(s). The width, thickness and spacing of the threads were 12 mm, 2 mm, and 50 mm, respectively. The Young's modulus and yield strength was calibrated by Guo and Deng (2018). The Young's modulus of the screw micropile material was 210 GPa and yield strength was 248 MPa.

Table 1. Dimensions of screw micropile

| Pile Type | Length (mm) (± 25mm) | Threaded Length (mm) (± 25mm) | Shaft diameter (mm) |
|---|---|---|---|
| P1 | 3075 | 2000 | 114.3 |
| P3 | 3070 | 2000 | 88.9 |
| P5 | 3078 | 1150 | 76.1 |

### 3.2 Load Test Configuration

The test setup is shown in Figure 3. The axial loading equipment included a 4.2 m long W360X179 I-beam fixed on top of the timber crippling and two sets of four 2.1 m long screw pile as reaction pile group with tension rods and bolts.

One of each pile types was instrumented with six strain gauge stations with either a half-bridge or a quarter-bridge Wheatstone circuit along its exterior shaft. The strain gauges were sealed with a layer of epoxy, a layer of aluminum foil, and a layer of blue clay and protected with a steel sheet casing as shown in Figure 4. A layer of blue clay, having very high permeability, was applied between the aluminum foil and steel sheet casing to provide waterproof for strain gauges below groundwater table. The steel sheet was bolted to the wall. The strain gauge measurement was used to calculate the axial internal load along the pile shaft.

Figure 3. Pile load test setup

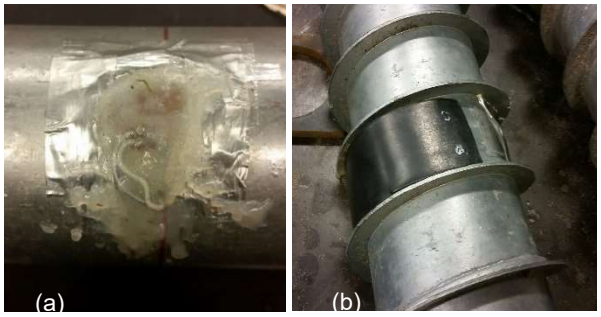


Figure 4. Strain gauge protection a) epoxy and aluminum foil, b) steel sheet casing

### 3.3 Test Summary

The compression and tension tests were done in accordance with ASTM standards D1143 (ASTM 2007a) and D3689 (ASTM 2007b), respectively. The quick test method or procedure A was followed. The capacities of the screw micropiles were estimated from first pile load test. The load steps were applied at 5% of the estimated capacity and maintained for 5 min. After plunging failure or excessive settlement had been reached, the load was reduced to zero reading in four equal steps.

In total, 22 full-scale load tests were performed on three types of screw micropiles. At least three compression tests and three tension tests were conducted on each pile type. The micropile identification, P1-C1* corresponds to the first compression test conducted on a screw micropile type P1 and the * symbol means that the test micropile was instrumented with strain gauge stations.

### 3.4 Linear Regression-Standard Penetration Method

Statistical relationships were derived between shaft resistance distributions and standard penetration value distributions using linear regression analysis. Regression coefficients were obtained for smooth, threaded and threaded-tapered segment separately. A linear relationship was defined where the mean value of unit shaft resistance ($q_{si}$) depended on a given value of SPT $N_{1,60}$ as follows:

$$E(q_{si} \mid N_{1,60} = N_{1,60}) = \alpha + \beta N_{1,60} = 0 + \beta N_{1,60} \quad [1]$$

where $\alpha$ is the intercept, $\beta$ is the slope of the linear line, $E$ is the mean value of the unit shaft resistance and $N_{1,60}$ is the SPT $N_{1,60}$ value. Given that shaft resistance of a pile segment would be zero in a soil with SPT $N_{1,60}$ value of zero, the intercept was assumed to be zero (i.e. $\alpha$=0). The best linear relationship was obtained by minimizing the squared least cumulative error between the linear line and the measured data as follows:

$$\Delta^2 = \sum_{i=1}^{n}(q_{s_i} - \grave{q}_{s_i})^2 = \sum_{i=1}^{n}(q_{s_i} - \beta N_{1,60_i})^2 \quad [2]$$

$$\frac{\partial \Delta^2}{\partial \beta} = \sum_{i=1}^{n} -2N_{1,60_i}(q_{s_i} - \beta N_{1,60_i}) = 0 \quad [3]$$

$$0 = \bar{q}_{si} - \beta \overline{N_{1,60_i}} \quad [4]$$

where $\Delta$ is the least cumulative error. Once the slope of the linear line was obtained, the ultimate capacities of the test piles were estimated using actual SPT $N_{1,60}$ value distribution, micropile geometry and micropile penetration.

## 4 RESULTS AND DISCUSSION

### 4.1 Load-Displacement Curves

The load-displacement curves of 22 test micropiles were processed as shown in Figures 5 to 7. The ultimate capacities of the screw test micropiles were calculated at the axial loads corresponding to an axial displacement equal to 10% of the shaft diameter. The average measured ultimate capacities ($Q_{u.ave}$) the number of tests and the coefficient of variations ($\delta$) of the test micropiles are summarized in Table 2.

As shown in Figures 5 to 7, the load-displacement curves of compression tests were ductile, whereas the load-displacement curves of tension tests were brittle. The ductile nature of compression test implies that mobilization of threaded-tapered capacity requires extensive tip displacement. The brittle nature of tension test curves implies the soil-pile slippage during the pullout. The load-displacement curves of compression tests continued with a modest rise at high axial displacements. The load displacement curves of tension tests declined after achieving a peak load at an axial displacement less than 20 percent of pile diameter. Therefore at the limit state, the compression capacities were greater than the tension capacities.

At the ultimate state, the compression and tension ultimate capacities were similar, where end bearing was not significantly mobilized. This similarity also implies that at the ultimate state, the majority of capacity may be sourced from the shaft resistance.

The variation of ultimate capacities and the load-displacement curves were affected by the variation of SPT $N_{1,60}$ value and soil disturbance due to variation in pile installation.

Table 2. Mean and coefficient of variations of the ultimate state capacity of test piles

| Pile Type | Test Type | $Q_{u.ave}$ (kN) | No. of tests | $\delta$ |
|---|---|---|---|---|
| P1 | C | 92 | 3 | 0.21 |
| P3 | C | 57 | 5 | 0.25 |
| P5 | C | 37 | 5 | 0.13 |
| P1 | T | 85 | 3 | 0.14 |
| P3 | T | 59 | 3 | 0.02 |
| P5 | T | 43 | 3 | 0.04 |

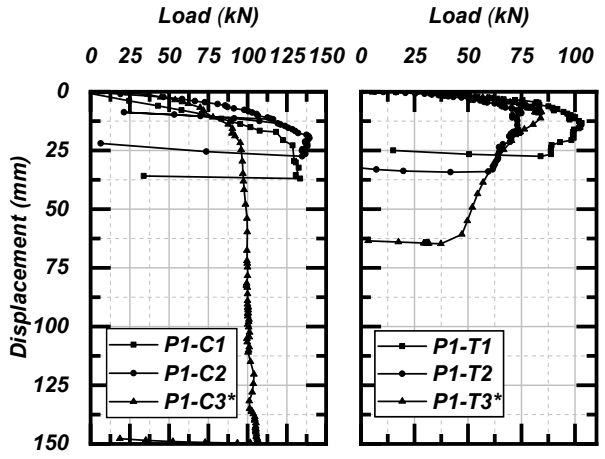


Figure 5. Load-displacement curves of pile P1 subjected to axial compression and tension. The start (*) symbol means instrumented piles.

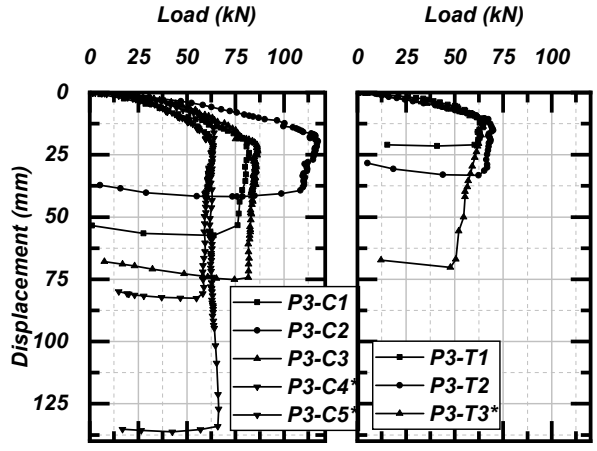


Figure 6. Load-displacement curve of pile P3 subjected to axial compression and tension

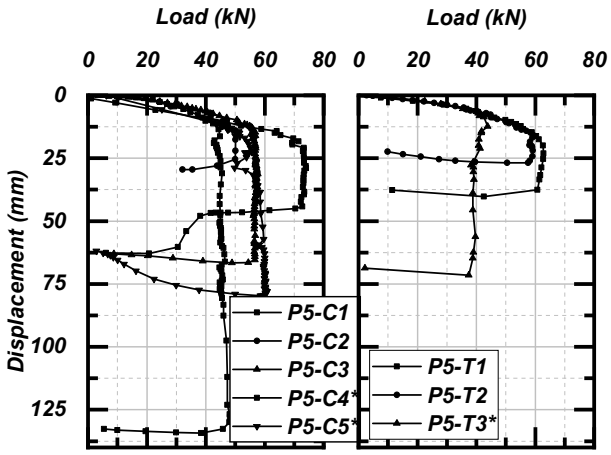


Figure 7. Load-displacement curve of pile P5 subjected to axial compression and tension

## 4.2 Unit Shaft Resistance

The instrumented pile test provides an opportunity to evaluate the unit shaft resistance of each micropile segment. The strain gauges were installed in such a manner to separate smooth segment, threaded segment, and threaded-tapered segment. The unit shaft resistances at the ultimate state, $q_s$, were then calculated as the differential load between gauges divided by the outer shaft area. In total, eight test micropiles were instrumented. Micropile P1 had one smooth, two threaded and two threaded-tapered instrumented segments. Micropile P3 had one smooth, three threaded, and one threaded tapered instrumented segment. Micropile P5 had two smooth, two threaded and one threaded-tapered instrumented segment. However, at some case, a pile segment was divided into two instrumented segment to obtain high resolution of unit shaft resistance. In total, there were eleven smooth, eleven threaded and ten threaded-tapered instrumented segments. The distributions of $q_s$ along eight instrumented micropiles depth are shown in Figure 8.

The statistical information including the number of samples (#), average shaft resistance $E(q_s)$, the minimum value of shaft resistance ($q_{s,min}$), the maximum shaft resistance ($q_{s,max}$), standard deviation ($\sigma$) and coefficient of variation ($\delta$) of each instrumented pile segments are shown in Table 3.

Table 3. Statistical information of measured unit shaft resistance of instrumented pile segment

| Shaft Segment | # | $E(q_s)$ (kPa) | $q_{s,min}$ (kPa) | $q_{s,max}$ (kPa) | $\sigma$ (kPa) | $\delta$ |
|---|---|---|---|---|---|---|
| Smooth | 11 | 61 | 15 | 101 | 23 | 0.38 |
| Threaded | 11 | 49 | 47 | 105 | 32 | 0.66 |
| Threaded-tapered | 10 | 149 | 146 | 339 | 113 | 0.76 |

The SPT $N_{1,60}$ value of the sand, segment type, soil disturbance due to pile installation and instrumentation had a contribution to the measured $q_s$. The SPT $N_{1,60}$ value of sand deposit across the site at three depth intervals had a mean and coefficient of variations of 25 and 0.12, 18 and 1.155, and 8.5 and 0.577 at three SPT locations, respectively. Therefore, the measured $q_s$ had a greater mean and coefficient of variation at higher elevations. And more generally, the measured $q_{s.smooth}$ and measured $q_{s.threaded}$ were greater in the upper sand sublayer compared to the lower sand sublayer. Generally at the soil with the same compactness and SPT $N_{1,60}$, the measured $q_{s.threaded}$ was greater than measured $q_{s.smooth}$ and the $q_{s.threaded\text{-}tapered}$ was greater than $q_{s.threaded}$. The mean measured $q_{s.threaded\text{-}tapered}$ was 304% greater than the measured $q_{s.threaded}$. At some instance, the contribution of the sand SPT $N_{1,60}$ value masks the contribution of the segment type to the $q_s$. Some of the variations of $q_s$ at the higher elevation could be due to the soil disturbance during pile installation.

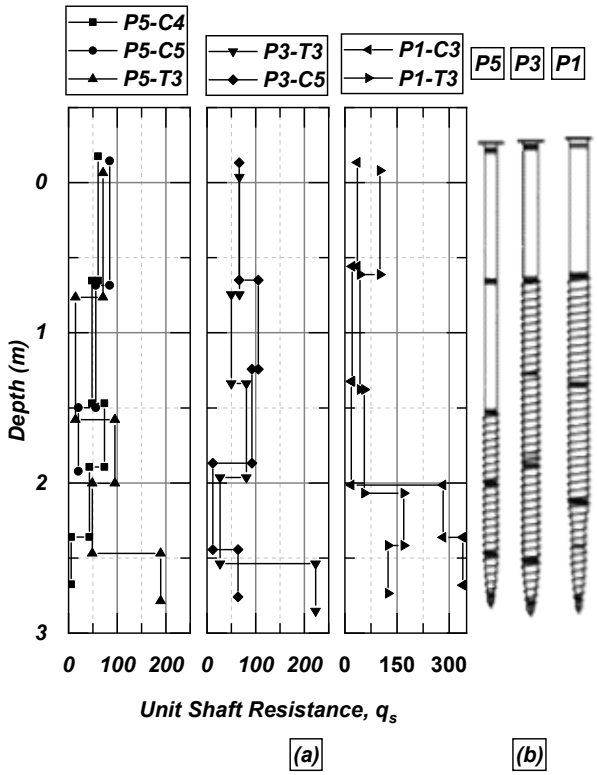


Figure 8. a) Distribution of unit shaft resistance $q_s$ at the ultimate state b) Screw micropile (Guo and Deng 2018)

4.3 Linear Regression-Standard Penetration Method

The measured $q_s$ and the corresponding SPT $N_{1,60}$ value of smooth, threaded and threaded-tapered instrumented segments are shown in Figures 9, 10 and 11, respectively. The statistical information including mean ($E(N_{1,60})$), standard deviation ($\sigma(N_{1,60})$), coefficient of variation ($\delta$), coefficient of correlation ($\rho$), linear regression coefficient ($\beta$) and standard deviation ($\sigma$)) of two correlated random variable $q_s$ and SPT $N_{1,60}$ value are shown in Table 4. The estimated $q_s$ and one standard deviation margins based on linear regression method are also shown in the figures.

Table 4. Statistical relationship of unit shaft friction and SPT $N_{1,60}$.

| | Smooth | Threaded | Threaded-tapered |
|---|---|---|---|
| $E(N_{1,60})$ | 20.4 | 16 | 9 |
| $\sigma(N_{1,60})$ | 0.24 | 3.873 | 0.49 |
| $\rho$ | 0.58 | 0.497 | 0.25 |
| $\beta$ (kPa) | 2.99 | 3.36 | 19.22 |
| $\sigma$ (kPa) | 24.27 | 27.75 | 113.24 |

Note: $\alpha = 0$ for the linear regression (refer to Equation 1)

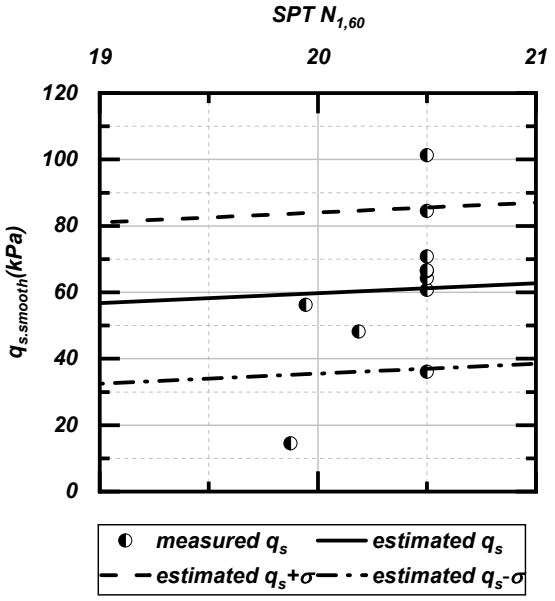


Figure 9. Correlation of measured smooth unit shaft resistance and SPT $N_{1,60}$ value

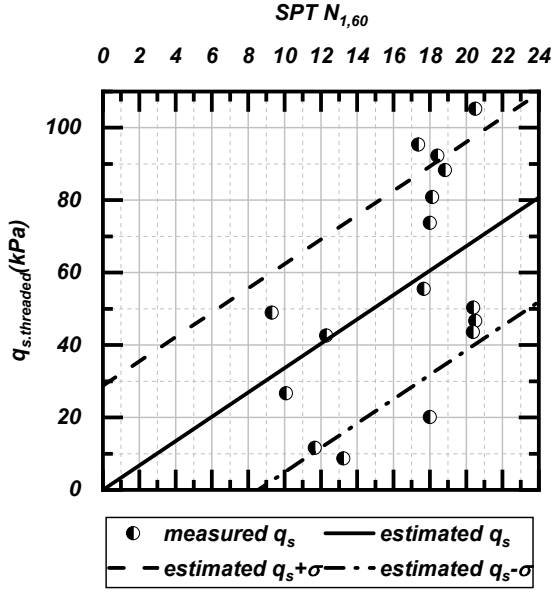


Figure 10. Correlation of measured threaded unit shaft resistance and SPT $N_{1,60}$ value

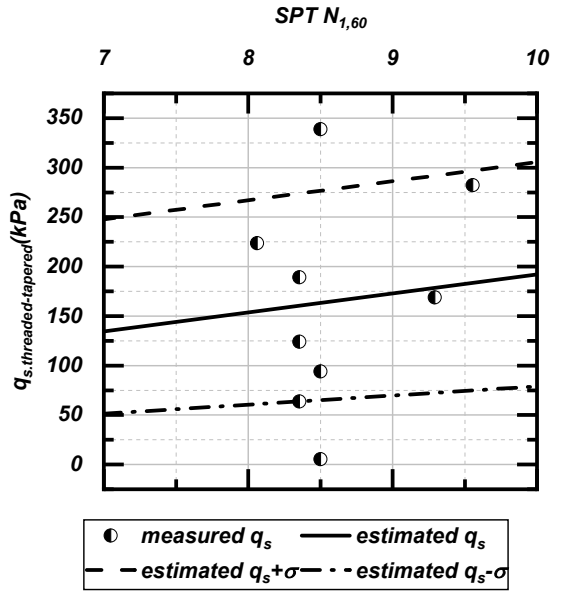


Figure 11. Correlation of measured threaded-tapered unit shaft resistance and SPT $N_{1,60}$ value

Given that denser sand exhibit greater $q_s$ and SPT-$N_{1,60}$ value, the $q_s$ and SPT $N_{1,60\ value}$ distribution generally both decrease with depth as the sand compactness condition changes from compact to loose. Linear regression method was used to correlate the measured $q_s$ and SPT $N_{1,60}$ values for smooth, threaded and threaded-tapered segment separately. Eight instrumented micropiles, consisted of P1, P3 and P5, were instrumented with strain gauges to obtain the $q_s$ distribution along the micropile length.

The slope of the linear relationship between the $q_{s.smooth}$, $q_{s.threaded}$, and $q_{s.threaded\text{-}tapered}$ and corresponding SPT $N_{1,60}$ were 2.99, 3.36 and 19.22, respectively. The regression coefficient obtained for smooth and threaded segments were comparable to values reported in literature by Briaud et al. (1983), Meyerhof (1956), Shariatmadari et al. (2008), Shioi and Fukui (1982), Thornburn and MacVicar (1971), Aoki and Velloso (1975), Brown (2001), Decourt (1982) and Decourt (1995). The difference between the regression coefficient values obtained in this research and the values posted in the literature may be due to the difference in micropile geometry and installation method. The regression coefficient value corresponding to the smooth and threaded segments of screw micropiles were closer to that obtained for driven piles by Decourt (1982). The lateral pressure on the screw micropile may be similar to a driven pile. Perhaps, the radial expansion of soil due to the screw micropile installation would result in high displacement similar to driven pile. Also, it was observed that the regression coefficient of the threaded segment is 112.5% greater than the smooth segment. This was due to the failure of soil along the threaded segment being further away from micropile shaft. The regression coefficient of the threaded-tapered was 643% greater than the smooth segment. This may be due to the increase capacity of tapered pile reported in Guo and Deng (2018).

### 4.4 Estimation of Ultimate Pile Capacity

The ultimate capacity of the screw micropile was estimated using derived regression coefficients, micropile geometry, pile penetration depth, and SPT $N_{1,60}$ value distribution as follows:

$$Q_u = \left( \sum_{i=0}^{10*L1} \beta_{sm.} + \sum_{i=10*L1}^{10*L2} \beta_{th.} + \sum_{i=L2*10}^{L3*10} \beta_{tap.} \right) N_{1,60_i} A_i \quad [5]$$

$$Q_u = \left( \sum_{i=0}^{10*L1} \beta_{sm.} + \sum_{i=10*L1}^{10*L2} \beta_{th.} + \sum_{i=L2*10}^{L3*10} \beta_{tap.} + \sum_{i=10*L3}^{10*L4} \beta_{th.} + \sum_{i=L4*10}^{L5*10} \beta_{tap.} \right) N_{1,60_i} A_i \quad [6]$$

where $Q_u$ is the estimated ultimate capacity, $N_{1,60}$ is the measured SPT $N_{1,60}$ value, $\beta_{sm.}$, $\beta_{th.}$, $\beta_{tap.}$ are the regression coefficients for the smooth, threaded and tapered segments respectively (refer to Table 4), and A is the outer area of pile segment. The ultimate capacities of 22 test micropiles were estimated as shown in Figure 11.

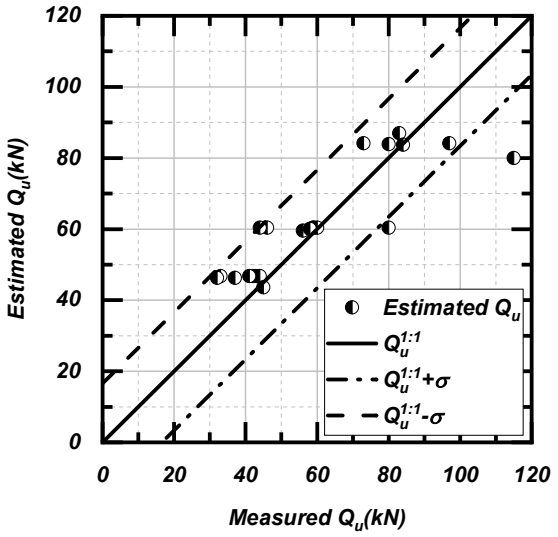


Figure 12. Measured and estimated ultimate capacities of screw micropiles tested for the present study

The correlation coefficient between estimated and measured $Q_u$ was 0.83, which seems to indicate that the accuracy of the estimation. The constant standard deviation of estimated ultimate capacities from the one-to-one ratio line of the estimated and measured ultimate capacities was 16 kN. The one-to-one ratio line and one constant standard deviation margins are also shown in Figure 12.

## 5 CONCLUSIONS

Twenty-two full-scale load tests were conducted on three types of screw micropile. Three screw micropiles were instrumented to obtain the distributions of unit shaft

resistance. The ultimate capacities were obtained from the load-displacement curve. The geotechnical site investigation showed that the surficial soil was composed of Aeolian sand. The compactness condition profile of the sand sublayer generally changes from compact to loose. And, the sand contains up to 20% gravel in the upper sand sublayer.

The load-displacement curves of compression tests were ductile and tension tests were brittle. The ductile nature of load-displacement curves of compression tests was due to the mobilization of the end bearing capacity. And the brittle nature of load-displacement curves of tension tests was due to the soil-pile slippage. At ultimate state, the compression and tension ultimate capacities were similar, where end bearing was not significantly mobilized. The majority of capacity of screw micropile comes from shaft resistance at ultimate state.

The measured unit shaft resistance had a greater mean and coefficient of variation at higher elevations. More generally, the measured smooth unit shaft resistance and measured threaded unit shaft resistance were greater in the upper sand sublayer compared to the lower sand sublayer. The measured threaded unit shaft resistance was greater than measured smooth unit shaft resistance and the threaded-tapered unit shaft resistance was greater than measured threaded unit shaft resistance. The mean measured threaded-tapered unit shaft resistance was 304% greater than the measured threaded unit shaft resistance. During pile installation, the micropiles were wobbled and the compact sand properties could have been altered to a state between the peak and the constant volume state. Better construction control can mitigate this.

Statistical relationships were developed between the shaft resistance distributions and SPT N values using linear regression analysis. Unit shaft resistance can be estimated using the equation: $q_s = \alpha + \beta N_{1,60}$, where $\alpha$ was set to zero and $\beta$ for smooth, threaded, and threaded and threaded-tapered segments were found to be 2.99, 3.36 and 19.22. The increase of linear regression coefficient in the threaded segment was due to the failure of soil along the threaded segment was further away from the pile shaft. The increase in the threaded-tapered segment was due to the mobilization of the end-bearing capacity.

Using the developed linear correlations between $q_s$ and $N_{1,60}$, the ultimate capacities of all test piles were estimated. The estimated values are comparable to the measured ultimate capacities, which suggests the feasibility of the developed correlations.

## AKNOWLEDGEMENTS

The present research is funded by Natural Science and Engineering Research Council of Canada (NSERC) with Collaborative R&D program with the financial support of Krinner Canada Inc. We very much appreciate the help of Tomas Johansson of Krinner. Field support was provided by Benoit Trudeau of Workonthat Structure Inc. for conducting the pile load tests.

## References

Aoki, N. and Velloso, D.D.A. 1975. An Approximate Method to Estimate the Bearing Capacity of Piles, In Proc., 5th Pan-American Conf. of Soil Mechanics and Foundation Engineering (Vol. 1, pp. 367-376), Buenos Aires: International Society of Soil Mechanics and Geotechnical Engineering.

American Society for Testing and Materials (ASTM). 2007. ASTM D1143-81, Standard Test Method for Deep Foundations Under Static Axial Compressive Load, ASTM International, West Conshohocken, PA, pp. 104–114

American Society for Testing and Materials (ASTM). 2007. ASTM D3689-07, Standard Test Methods for Deep Foundations Under Static Axial Tensile Load, Annual Book of ASTM Standards, Vol. 04.08, ASTM International, West Conshohocken, PA, pp. 405–423.

Bayrock, L.A. 1958. Glacial geology, Galahad-Hardisty district, Alberta, Vol. 57, No. 3, Research Council of Alberta.

Briaud, J.L., Tucker, L., Lytton, R.L. and Coyle, H.M.. 1985. Behavior of piles and pile groups in cohesionless soils (No. FHWA-RD-83-038).

Brown, R. P. 2001. Predicting the Ultimate Axial Resistance of Single Driven Piles, Ph. D. thesis, University of Texas, Austin, Texas, USA.

Cadden, A., Gomez, J., Bruce, D. and Armour, T. 2004. Micropiles: Recent Advances and Future Trends. In: Current Practices and Future Trends in Deep Foundations, ASCE Geotechnical Special Publication, (125).

Decourt, L. 1982. Prediction of the Bearing Capacity of Piles Based Exclusively on N values of the SPT. In Proceedings of the 2nd European Symposium, Vol. 1, pp. 29-34.

Decourt, L. 1995. Prediction of Load Settlement Relationships for Foundations on the Basis of the SPT-T, Ciclo de Conferencias Internationale, Leonardo Zeevaert, UNAM, Mexico, 85-104.

Fenton, M.M., Moran, S.R., Teller, J.T. and Clayton, L. 1983. Quaternary Stratigraphy and History in the Southern Part of the Lake Agassiz Basin, In Glacial Lake Agassiz, Vol. 26, pp. 49-74, St. John's: Geological Association of Canada.

Guo, Z. and Deng, L. 2018. Field Behaviour of Screw Micropiles Subjected to Axial Loading in Cohesive Soils, Canadian Geotechnical Journal, 55(1), pp.34-44.

Guo, Z., Khidri, M. and Deng, L. 2018. Field Loading Tests of Screw Micropiles under Axial Cyclic and Monotonic Loads, Acta Geotechnica, pp.1-14.

Hoyt, R. M. 1989. Uplift Capacity of Helical Anchors on Soil, Proceedings of 12th International Conference on Soil Mechanics and Foundation Engineering.

Juran, I., Bruce, D.A., Dimillio, A. and Benslimane, A. 1999. Micropiles: The State of Practice. Part II: Design of Single Micropiles and Groups and Networks of Micropiles, Proceedings of the Institution of Civil Engineers-Ground Improvement, 3(3), pp.89-110.

Ladanyi, B., and A. Guichaoua. 1985. Bearing Capacity and Settlement of Shaped Piles in Permafrost, Proceedings of the Eleventh International Conference

on Soil Mechanics and Foundation Engineering, San Francisco, 12-16, Publication of: Balkema (AA).

Meyerhof, G. G. 1956. Penetration Tests and Bearing Capacity of Cohesionless Soils, Journal of the Soil Mechanics and Foundations Division, 82(1), 1-19.

Sabatini, P.J., Tanyu, B., Armour, T., Groneck, P. and Keeley, J. 2005. Micropile Design and Construction. US Department of Transportation, Federal Highway Administration, Washington, DC, Report No. FHWA-NHI-05-039.

Shariatmadari, N., Eslami, A.A. and Karim, P.F.M. 2008. Bearing Capacity of Driven Piles in Sands from SPT–Applied to 60 Case Histories. Iranian Journal of Science and Technology, 32(B2):25-140.

Shioi, Y. and Fukui, J. 1982. Application of N-value to Design of Foundations in Japan, In Proceeding of the Second European Symposium on Penetration Testing, Vol. 1, No. 1982, pp. 159-16.

Thorburn, S. and MacVicar, R.S.L. 1971. Pile Load Tests to Failure in the Clyde alluvium, In Behaviour of Piles (pp. 1-7), Thomas Telford Publishing.